Research Journal of Agricultural Science, 57 (4), 2025; ISSN: 2668-926X;

http://doi.org/10.59463/RJAS.2025.4.58

MOUNTAIN AREA CHARACTERIZATION BASED ON DEM AND SLOPE BY REMOTE SENSING

Anda VUȘCAN[1], M. AVĂDANEI[1], I. VETO[1], Florina ȚÂRLE BURESCU[1], F. SALA[2,3], M.V. HERBEI[1,2]

[1]University of Petrosani, 332006, University Street, nr. 20, Petroșani, Romania

[2]University of Life Sciences "King Mihai I" from Timisoara, 300645, 119, Calea Aradului, Timisoara, Romania

[3]Agricultural Research and Development Station Lovrin, 307250, Lovrin, Romania

Corresponding author: florin_sala@usvt.ro

Abstract. *Remote sensing is very useful in the study and characterization of terrestrial areas based on satellite images and specific indices. The present study aimed to characterize an area using remote sensing facilities. The study considered ATU Lupsa, Alba County, Romania, an area with mountainous area specificity. DEM (Digital Elevation Model) and SLOPE parameters were used to analyze and characterize the area considered in the study. Land areas with different soil types were identified in terms of texture, Clayey loam texture (CLt), Clay texture (Ct), Sandy clay texture (SCt), Sandy loam - clayey texture (SLCt), and Varied texture (Vt). The studied area was classified based on DEM and SLOPE parameters into ten classes. Multivariate analysis (PCA, CA) was used to explain the variance in the results set and the correlation of DEM and SLOPE classes with soil types. In the case of the DEM parameter, PC1 explained 57.044% of variance, and PC2 explained 25.803%. In the case of the SLOPE parameter, PC1 explained 41.406% of variance, and PC2 explained 37.572% of variance. Cluster analysis (CA) grouped the DEM (Coph.corr. = 0.982) and SLOPE (Coph.corr. =0.781) classes based on similarity. The highest level of similarity in the case of DEM was recorded between classes DC4 and DC5, with the SDI value = 60.28, and in the case of SLOPE it was recorded between classes SC4 and SC5, with the SDI value = 99.87. The recorded results provide important information for management decisions for the area considered.*

Keywords: *cluster, DEM, PCA, remote sensing, SLOPE*

INTRODUCTION

The study of terrestrial areas has benefited substantially from remote sensing facilities, through high-resolution images, the calculation of specific indices, the generation of models, the provision of information in data format and maps for the description of areas considered of interest (MAO ET AL., 2020; GADAL AND MOZGERIS, 2025; SABAGHY ET AL., 2025).

Remote sensing has been used for monitoring natural and anthropogenic areas, for analyzing land changes, for evaluating agricultural lands and crops (HERBEI AND SALA, 2020; ZHU ET AL., 2022; BAIRWA ET AL., 2025).

DEM (Digital Elevation Model) is of great importance in remote sensing and the study of land areas. DEM is a representation of the topography of the land surface (an area, a landscape) in digital format, without including surface elements or objects in the representation (OKOLIE AND SMIT, 2022; MOHAMED ET AL., 2024).

SLOPE is an important parameter in remote sensing for the study of terrestrial areas, to describe the geometry of the slopes of the analyzed areas (VANNESCHI ET AL., 2017; WANG ET AL., 2024).

Mountain areas are characterized by a specific typology, with high spatial variability, and remote sensing has been a very useful tool for scanning, analyzing and characterizing these types of areas (HERBEI AND SALA, 2014; NAN ET AL., 2024; BIAN ET AL., 2025; YANG ET AL., 2025).

Research Journal of Agricultural Science, 57 (4), 2025; ISSN: 2668-926X;

http://doi.org/10.59463/RJAS.2025.4.58

In studies of analysis, characterization and classification of mountain areas, DEM was used in remote sensing techniques (CHYMYROV, 2021; JOMBO ET AL., 2023; ZHAO ET AL., 2023). SLOPE was monitored to characterize mountain areas, in relation to ecosystem and economic elements (QIN ET AL., 2020; YIN ET AL., 2022; WANG ET AL., 2023).

DEM and SLOPE data have been used in land characterization, classification, clustering and segmentation studies to highlight land conditions, stability and vulnerability areas (IWAHASHI ET AL., 2018; IWAHASHI ET AL., 2021; ZHANG ET AL., 2025).

The present study aimed to characterize a mountainous area, represented by ATU Lupsa, Alba County, Romania, based on DEM and SLOPE parameters generated through remote sensing technique.

MATERIAL AND METHODS

The study area was represented by ATU Lupsa, Alba County, Romania. ATU Lupsa is located in Alba County, in the historical region of Transylvania, Romania. The commune includes 23 villages in its administrative structure: 'Bârdești', 'Bârzan', 'Curmătură', 'După Deal', 'Geamăna', 'Hădărău', 'Holobani', 'Lazuri', 'Lunca', 'Lupșa', 'Mănăstire', 'Mărgaia', 'Mușca', 'Pârâu-Cărbunări', 'Pițiga', 'Poșogani', 'Șasa', 'Trifești', 'Văi', 'Valea Holhorii', 'Valea Lupșii', 'Valea Șesii' and 'Vința'.

The locality of Lupșa is located on the northern slopes of the 'Muntelui Mare' and the southern slopes of the 'Muntilor Metaliferi', Figure 1, generated based on ArcGIS (ESRI, 2011). The relief is predominantly mountainous, formed on crystalline schists and metalliferous rocks. The altitude varies from 550 m in the 'Aries' River meadow, which crosses the commune for a distance of 19 km, reaching up to 1,350 m in the 'Geamana' area.

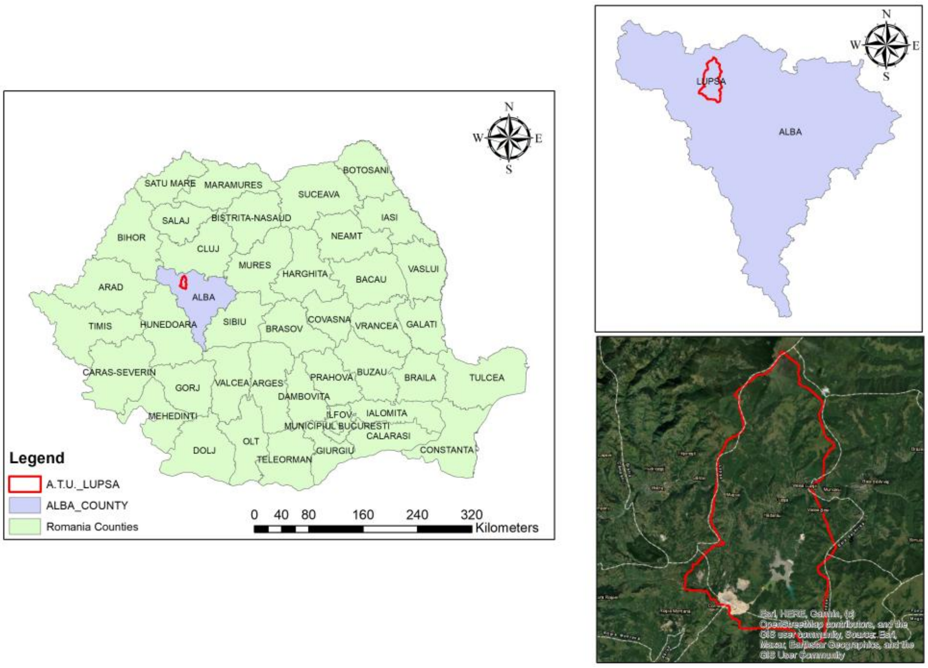

Figure 1. Study location, ATU Lupsa, Alba County, Romania

http://doi.org/10.59463/RJAS.2025.4.58

Economic activities specific to the area are: Mining, Agriculture, Animal Husbandry, Forestry and Construction (https://ghidulprimariilor.ro/).

Within the Lupsa ATU is the Roșia Poieni mining operation, which is a surface copper operation in the Apuseni Mountains, located 90 km northwest of Alba Iulia and 7 km south of the Aries River. The quarry began operating in 1978, in the Abrud-Musca-Bucium area of the Apuseni Mountains, with copper production starting in 1983. It is the largest disseminated copper and gold deposit in Romania, with its reserves representing 65% of the total copper in Romania. The mine produces ore from which approximately 5,000 tons of copper can be extracted per year.

Based on satellite images, the values of DEM and SLOPE parameters were determined to characterize the study area. The classification of the studied area was made on ten DEM and SLOPE classes. Also, the soil categories were evaluated in relation to texture, on the textural classes Clayey loam texture (CLt), Clay texture (Ct), Sandy clay texture (SCt), Sandy loam - clayey texture (SLCt), Varied texture (Vt), based on ICPA (https://icpa.ro/harti-sol/). The total area of the study area was determined, and the area for each soil texture category, in relation to the DEM and SLOPE classes.

Recorded data were analyzed mathematically and statistically to evaluate the correlation of parameters in relation to the principal components. The level of similarity at the level of recorded classes (DEM, SLOPE), in relation to soil texture, as an action factor, was evaluated. The PAST software (HAMMER ET AL., 2001) was used for the processing and statistical analysis of experimental data and the generation of figures and graphs.

RESULTS AND DISCUSSIONS

The analysis of the study area based on DEM and SLOPE parameters, corroborating the surface occupied by different soil types by textural class (CLt, Ct, SCt, SLCt, and Vt) resulted in the surface data (ha) presented in Table 1 (DEM parameter classes) and Table 2 (SLOPE parameter classes).

Table 1

Distribution of land surfaces by DEM classes in the study area

DEM Class	CLt	Ct	SCt	SLCt	Vt	Area
	(ha)					
DC1	0	186.08	292.13	268.54	458.29	1205.04
DC2	0	99.2	1082.94	300.99	39.19	1522.32
DC3	0	69.31	1551.11	143.9	0.22	1764.54
DC4	0.46	42.78	1547.92	37.93	0	1629.09
DC5	19	23.53	1509.44	0	0	1551.97
DC6	20.63	5.95	1373.73	0	0	1400.31
DC7	6.45	0	977.26	0	0	983.71
DC8	0	0	492.05	0	0	492.05
DC9	0	0	322.35	0	0	322.35
DC10	0	0	179.92	0	0	179.92
Grand Total	46.54	426.85	9328.85	751.36	497.7	11051.3

Research Journal of Agricultural Science, 57 (4), 2025; ISSN: 2668-926X;
http://doi.org/10.59463/RJAS.2025.4.58

Table 2

Distribution of land surfaces by SLOPE classes in the study area

SLOPE Class	CLt	Ct	SCt	SLCt	Vt	Area
	(ha)					
SC1	0	55.44	197.11	92.13	269.88	614.56
SC2	0.82	47.54	730.15	140.04	40.12	958.67
SC3	1.93	51.76	1358.24	185.36	26.9	1624.19
SC4	4.44	44.93	1612.74	163.03	21.95	1847.09
SC5	6.11	43.86	1534.96	100.46	24.33	1709.72
SC6	8.49	51.7	1333.18	47.79	24.43	1465.59
SC7	11.57	47.94	1109.62	16.36	22.8	1208.29
SC8	8.53	38.39	792.75	4.16	26.14	869.97
SC9	4.14	30.17	497.19	2.03	24.28	557.81
SC10	0.51	15.12	162.91	0	16.87	195.41
Grand Total	46.54	426.85	9328.85	751.36	497.7	11051.3

The multivariate analysis explained the correlation between the classes related to the DEM and SLOPE parameters and the land surface based on soil textural categories in the study area. In the case of the DEM parameter, PC1 explained 57.044% of variance, and PC2 explained 25.803% of variance, Figure 2. The correlation of some DEM classes with soil textural classes was observed, and the independent positioning of other DEM classes in which soil textural classes were not found. The graphical representation of the Component – Eigenvalue interaction is presented in Figure 3.

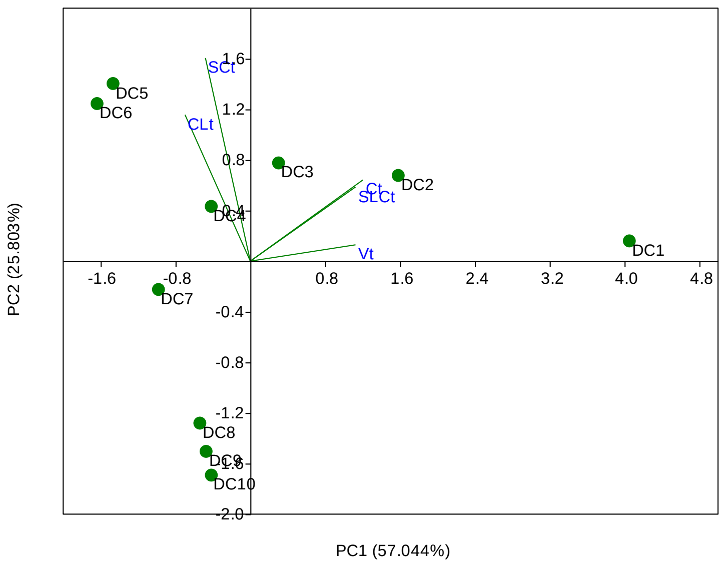

Figure 2. PCA diagram in relation to DEM parameter

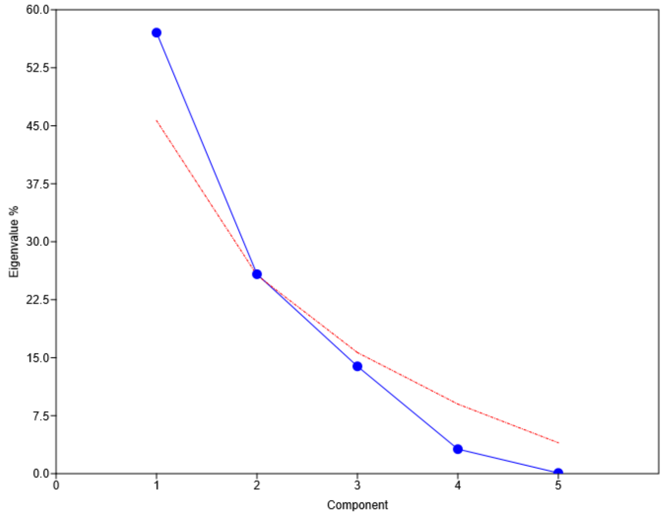

Figure 3. Graphical representation of the Component – Eigenvalue interaction in the case of DEM classes

The score of the DEM classes in relation to the Principal Components is presented in Table 3. In PC1, the DC1 class presented a high value, in PC2, the DC5 class presented a high value, in PC3, the DC1 class presented a high value, in PC4, the DC2 class presented a high value, and in PC5, the DC7 class presented a high value. The factor loading (soil texture type) in the principal components is presented in Table 4.

Table 3

DEM class score in Principal Components

DEM Classes	PC 1	PC 2	PC 3	PC 4	PC 5
DC1	4.0515	0.1602	1.1366	-0.2678	0.0052
DC2	1.5811	0.6781	-1.0981	0.8145	0.0156
DC3	0.3019	0.7769	-1.1907	-0.2234	-0.0281
DC4	-0.4178	0.4333	-0.8845	-0.7228	-0.0092
DC5	-1.4674	1.4043	0.7430	0.0253	-0.1023
DC6	-1.6379	1.2459	0.9720	0.2503	0.0492
DC7	-0.9822	-0.2237	0.1136	-0.1075	0.1394
DC8	-0.5395	-1.2803	-0.0499	-0.0451	0.0353
DC9	-0.4729	-1.5037	0.0761	0.0841	-0.0266
DC10	-0.4169	-1.6911	0.1819	0.1924	-0.0787

Table 4

Factor loadings in the principal components, in relation to DEM classes

Soil texture	PC 1	PC 2	PC 3	PC 4	PC 5
CLt	-0.3222	0.5342	0.6695	0.3922	-0.0934
Ct	0.5555	0.2965	0.0144	-0.1534	-0.7615
SCt	-0.2213	0.7416	-0.4183	-0.4287	0.2058
SLCt	0.5191	0.2707	-0.3084	0.6662	0.3440
Vt	0.5189	0.0599	0.5305	-0.4416	0.5008

In PC 1, Ct showed a high value, in PC 2, SCt showed a high value, in PC 3, CLt showed a high value, in PC 4, SLCt showed a high value, and in PC 5, Vt showed a high value.

In the case of the SLOPE parameter, PC1 explained 41.406% of variance, and PC2 explained 37.572% of variance, Figure 4. The independent positioning of classes SC8, SC9 and SC10 was observed, and the other SLOPE classes were positioned correlated with the soil texture types in the study area, depending on the class classification. The graphical representation of the Component – Eigenvalue interaction in the case of SLOPE classes is presented in Figure 5.

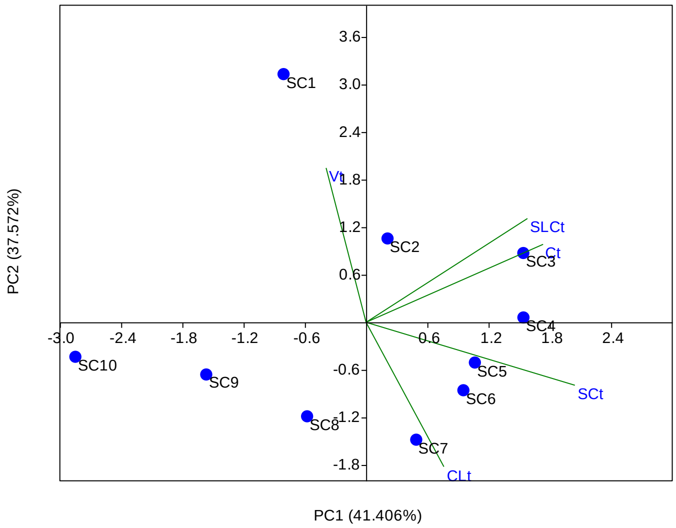

Figure 4. PCA diagram in relation to the SLOPE parameter

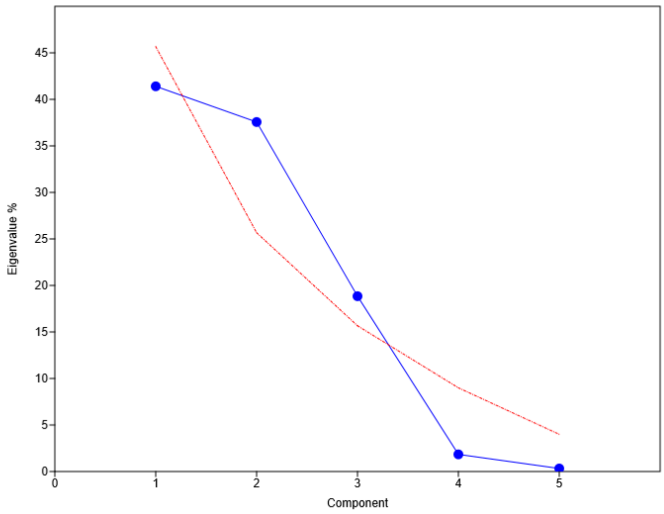

Figure 5. Representation of the Component – Eigenvalue interaction in the case of SLOPE classes

Research Journal of Agricultural Science, 57 (4), 2025; ISSN: 2668-926X;
http://doi.org/10.59463/RJAS.2025.4.58

The SLOPE class score in relation to the Principal Components is presented in Table 5. In PC1, the SC4 class presented a high value, in PC2, the SC1 class presented a high value, in PC3, the SC1 class presented a high value, in PC4, the SC5 class presented a high value, and in PC5, the SC7 class presented a high value. The factor loading (soil texture type) in the principal components is presented in Table 6.

Table 5

SLOPE class score in Principal Components

	PC 1	PC 2	PC 3	PC 4	PC 5
SC1	-0.8089	3.1314	1.4107	0.2010	0.0044
SC2	0.2102	1.0581	-0.7632	-0.5904	0.0363
SC3	1.5401	0.8740	-0.9973	-0.1988	-0.0098
SC4	1.5413	0.0612	-0.8720	0.3952	0.1330
SC5	1.0657	-0.5075	-0.2503	0.4235	-0.0901
SC6	0.9532	-0.8573	0.7633	-0.1072	-0.2657
SC7	0.4912	-1.4808	1.2947	-0.1460	0.1671
SC8	-0.5782	-1.1861	0.6999	-0.0607	0.1176
SC9	-1.5662	-0.6580	-0.1350	-0.0713	-0.0957
SC10	-2.8484	-0.4350	-1.1508	0.1547	0.0030

Table 6

Factor loadings in the principal components, in relation to SLOPE classes

	PC 1	PC 2	PC 3	PC 4	PC 5
CLt	0.2361	-0.5642	0.5462	0.0429	0.5708
Ct	0.5372	0.3047	0.4585	-0.5542	-0.3180
SCt	0.6335	-0.2460	-0.1475	0.5912	-0.4085
SLCt	0.4895	0.4056	-0.4469	-0.0330	0.6285
Vt	-0.1214	0.6032	0.5196	0.5834	0.1053

In PC1, a high value was shown for SCt, in PC2, a high value was shown for Vt, in PC3, a high value was shown for CLt, in PC4, a high value was shown for SCt, and in PC5, a high value was shown for SLCt.

Cluster analysis grouped the DEM and SLOPE parameter classes based on similarity in relation to the area of each class, given by the soil texture in the study area. In the case of DEM, cluster analysis led to the dendrogram in Figure 6 (Coph.corr. = 0.892). The DEM classes were grouped into two clusters, with several subclusters each. The highest level of similarity was recorded in the case of classes DC4 and DC5, with the SDI value = 60.28. The SDI values for the DEM classes are presented in Table 7.

In the case of SLOPE, the cluster analysis led to the dendrogram in Figure 7 (Coph.corr. = 0.781). The SLOPE classes were grouped in two balanced clusters, five classes in each cluster, with several subclusters each. The highest level of similarity was recorded in the case of classes DC4 and DC5, with the SDI value = 99.87. The SDI values for the SLOPE classes are presented in Table 8.

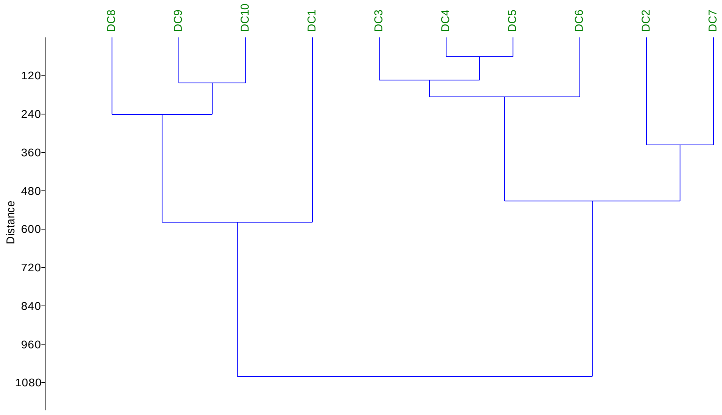

Figure 5. Cluster dendrogram for DEM parameter

Table 7

SDI values for DEM classes

	DC1	DC2	DC3	DC4	DC5	DC6	DC7	DC8	DC9	DC10
DC1		899.79	1350.60	1364.10	1338.20	1218.60	886.69	597.27	563.63	573.90
DC2	899.79		496.26	538.63	529.26	431.06	336.42	671.66	824.91	957.82
DC3	1350.60	496.26		109.29	157.80	237.93	595.70	1071.00	1239.10	1380.50
DC4	1364.10	538.63	109.29		60.28	183.15	573.55	1057.40	1226.90	1369.20
DC5	1338.20	529.26	157.80	60.28		136.85	532.85	1017.80	1187.50	1329.90
DC6	1218.60	431.06	237.93	183.15	136.85		396.77	881.94	1051.60	1194.00
DC7	886.69	336.42	595.70	573.55	532.85	396.77		485.25	654.94	797.37
DC8	597.27	671.66	1071.00	1057.40	1017.80	881.94	485.25		169.70	312.13
DC9	563.63	824.91	1239.10	1226.90	1187.50	1051.60	654.94	169.70		142.43
DC10	573.90	957.82	1380.50	1369.20	1329.90	1194.00	797.37	312.13	142.43	

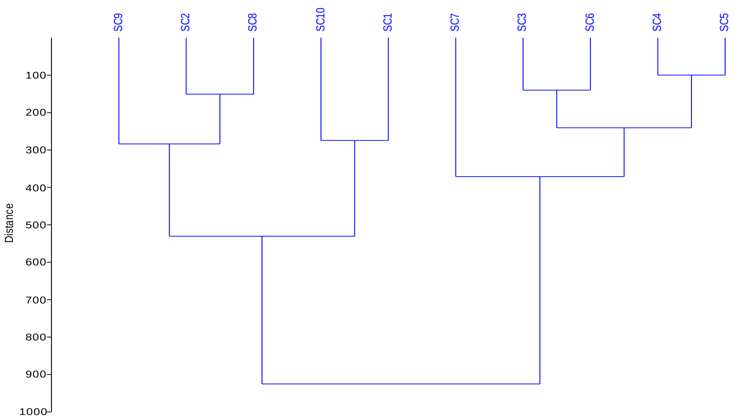

Figure 6. Cluster dendrogram for the SLOPE parameter

Table 8

SDI values for SLOPE classes

	SC1	SC2	SC3	SC4	SC5	SC6	SC7	SC8	SC9	SC10
SC1		582.48	1189.90	1439.00	1360.30	1163.20	948.50	649.84	398.92	274.40
SC2	582.48		629.88	883.09	805.96	610.31	399.64	150.73	271.81	585.63
SC3	1189.90	629.88		255.63	196.28	140.01	300.83	594.00	880.62	1210.20
SC4	1439.00	883.09	255.63		99.87	302.49	524.12	835.28	1127.20	1459.30
SC5	1360.30	805.96	196.28	99.87		208.70	433.63	748.46	1042.50	1376.10
SC6	1163.20	610.31	140.01	302.49	208.70		225.82	542.35	837.53	1171.90
SC7	948.50	399.64	300.83	524.12	433.63	225.82		317.28	612.90	947.50
SC8	649.84	150.73	594.00	835.28	748.46	542.35	317.28		295.72	630.40
SC9	398.92	271.81	880.62	1127.20	1042.50	837.53	612.90	295.72		334.73
SC10	274.40	585.63	1210.20	1459.30	1376.10	1171.90	947.50	630.40	334.73	

CONCLUSIONS

Remote sensing provided reliable information through DEM and SLOPE parameters for the description of the ATU Lupsa area, Alba County, Romania. The generated DEM and SLOPE classes included variable land areas in relation to the soil textural class.

Multivariate analysis (PCA) explained the variance in the experimental dataset and showed the correlation of DEM and SLOPE classes with soil texture types across the land surfaces recorded in the study area.

Cluster analysis grouped the DEM and SLOPE classes based on similarity, in relation to the land surfaces or soils of a certain texture, classified in each class.

The results provided by this study recommend the development of research for the area considered, the diversification of characterization indices, in order to provide information and solutions for management decisions.

BIBLIOGRAPHY

BAIRWA, B., SHARMA, R., KUNDU, A., SAMMEN, S.S., ALSHEHRI, F., PANDE, C.B., ORBAN, Z., SALEM, A., 2025 - Predicting changes in land use and land cover using remote sensing and land change modeler. Frontiers in Environmental Science, 13: 1540140.

BIAN, J., ZHAO, J., LI, A., 2025 - Remote sensing monitoring of mountain sustainable development goals (SDG15.4): a systematic review. International Journal of Digital Earth, 18(1): 2448216.

CHYMYROV A., 2021 - Comparison of different DEMs for hydrological studies in the mountainous areas. The Egyptian Journal of Remote Sensing and Space Science, 24(3, Part 2): 587-594.

ESRI, 2011 - ArcGIS Desktop: Release 10. Redlands, CA: Environmental Systems Research Institute.

GADAL, S., MOZGERIS, G., 2025 - Advances of remote sensing in land cover and land use mapping. Remote Sensing, 17(12): 1980.

HAMMER, Ø., HARPER, D.A.T., RYAN, P.D., 2001 - PAST: Paleontological Statistics software package for education and data analysis. Palaeontologia Electronica, 4(1): 1-9.

HERBEI, M.V., SALA, F., 2014 - Using GIS technology in processing and analyzing satellite images-case study Cheile Nerei Beusnița National Park, Romania. Journal of Horticulture, Forestry and Biotechnology, 18(4): 113-119.

HERBEI, M.V., SALA, F., 2020 - Evaluation of urban areas by remote sensing methods in relation to climatic conditions: Case study City of Timisoara. Carpathian Journal of Earth and Environmental Sciences, 15(2): 327-337.

IWAHASHI, J., KAMIYA, I., MATSUOKA, M., YAMAZAKI, D. 2018 - Global terrain classification using 280 m

DEMs: segmentation, clustering, and reclassification. Progress in Earth Planetary Science, 5: 1.

IWAHASHI, J., YAMAZAKI, D., NAKANO, T., ENDO, R., 2021 - Classification of topography for ground vulnerability assessment of alluvial plains and mountains of Japan using 30 m DEM. Progress in Earth Planetary Science, 8: 3.

JOMBO, S., ABD ELBASIT, M.A.M., GUMBO, A.D., NETHENGWE, N.S., 2023 - Remote sensing application in mountainous environments: A bibliographic analysis. International Journal of Environmental Research Public Health, 20(4): 3538.

MAO, L., LI, M., SHEN, W., 2020 - Remote sensing applications for monitoring terrestrial protected areas: Progress in the last decade. Sustainability, 12(12): 5016.

MOHAMED, A.H., KESKES, M.I., NITA, M.D., 2024 - Analyzing the accuracy of satellite-derived DEMs using high-resolution terrestrial LiDAR. Land, 13(12): 2171.

NAN, X., LI, A., BIAN, J., ZHANG, Z., LEI, G., 2024 - Morphological mapping of mountains on a global scale: combining topographic representation with tectonic features. Journal of Maps, 21(1): 2442708.

OKOLIE, C.J., SMIT, J.L., 2022 - A systematic review and meta-analysis of Digital elevation model (DEM) fusion: pre-processing, methods and applications. ISPRS Journal of Photogrammetry and Remote Sensing, 188: 1-29.

QIN, Y., HOPPE, E., PERISSIN, D., 2020 - Slope hazard monitoring using high-resolution satellite remote sensing: Lessons learned from a case study. ISPRS International Journal of Geo-Information, 9(2): 131.

SABAGHY, S., ABUZAR, M., CRAWFORD, D., LCALLISTER, A., SHEFFIELD, K., 2025 - Remote sensing for land cover mapping across Victoria, Australia – a machine learning application. Scientific Data, 12: 566.

VANNESCHI, C., EYRE, M., FRANCIONI, M., COGGAN, J., 2017 - The use of remote sensing techniques for monitoring and characterization of slope instability. Procedia Engineering, 191: 150-157.

WANG, X., LIU, G., XIANG, A., XIAO, S., LIN, D., LIN, Y., LU, Y., 2023 - Terrain gradient response of landscape ecological environment to land use and land cover change in the hilly watershed in South China. Ecological Indicators, 146: 109797.

WANG, X., HONDA, H., DJAMALUDDIN, I., TANIGUCHI, H., MITANI, Y., 2024 - Quantitatively detecting ground surface changes of slope failure caused by heavy rain using ALOS-2/PALSAR-2 data: a case study in Japan. Scientific Reports, 14: 23110.

YANG, X., LI, S., MA, J., CHEN, Y., ZHOU, X., LI, F., XIOUNG, L., ZHOU, C., TANG, G., MEADOWS, M.E., 2025 - A typology of global relief classes derived from digital elevation models at 1 arcsec resolution. Earth System Science Data, 17: 4331-4350.

YIN, H., CHEN, C., DONG, Q., ZHANG, P., CHEN, Q., ZHU, L., 2022 - Analysis of spatial heterogeneity and influencing factors of ecological environment quality in China's North-South transitional zone. International Journal of Environmental Research and Public Health, 19(4): 2236.

ZHANG, Y., SUN, J., LU, Y., 2025 - Mountain-valley geomorphological classification and agricultural land use in Southwest China. Ecological Indicators, 178: 113928.

ZHAO, MW., FANG, Y., YANG, CC., JU, XX., HUANG, ZI., JIANG, L., WANG, C., XU, Y., 2023 - Peak extraction and classification from digital elevation models based on the relationship between morphological characteristics and spatial position. Journal of Mountain Science, 20: 2015-2028.

ZHU, Z., QIU, S., YE, S., 2020 - Remote sensing of land change: A multifaceted perspective. Remote Sensing of Environment, 282: 113266.

https://ghidulprimariilor.ro/ro/businesses/view/city_hall/PRIMARIA-LUPSA/129451

https://icpa.ro/harti-sol/